ANALYSIS OF THE STABILITY OF THE LINEAR BOUNDARY CONDITION FOR THE BLACK-SCHOLES EQUATION.*

H. WINDCLIFF†, P.A. FORSYTH‡, AND K.R. VETZAL§

Abstract. The linear asymptotic boundary condition, i.e. assuming that the second derivative of the value of the derivative security vanishes as the asset price becomes large, is commonly used in practice. To our knowledge, there have been no rigorous studies of the stability of these methods, despite the fact that the discrete matrix equations obtained using this boundary condition loses diagonal dominance for large timesteps. In this paper, we demonstrate that the discrete equations obtained using this boundary condition satisfy necessary conditions for stability for a finite difference discretization. Computational experiments also show that this boundary condition satisfies sufficient conditions for stability as well.

Keywords: Asymptotic boundary condition, stability, finite difference, Black-Scholes equation

Revised October 24, 2003

1. Motivation. When solving option pricing PDEs such as the Black-Scholes equation numerically, many authors [19, 18, 10] have recommended a linear asymptotic boundary condition (that the second derivative of the option value with respect to the underlying asset value be zero) as the asset price becomes large. Although this boundary specification is often applied, to our knowledge there have been no rigorous studies of the stability of this technique. Looking at the form of the discrete matrix equations obtained using this boundary condition, the resulting discrete equations lose diagonal dominance for large timesteps and the usual arguments cannot be applied to guarantee unconditional stability.

In order to determine the ranges of parameters (risk-free rate, volatility, etc.) for which this asymptotic boundary condition could cause instability, we derive necessary conditions for the stability of the discrete equations based on the spectrum of the matrix representing the spatial discretization. Somewhat surprisingly, we find that a finite difference (FD) discretization always satisfies these necessary conditions for stability, despite the fact that the matrix equations are not unconditionally diagonally dominant.

The eigenvalues can be used to determine necessary conditions for stability but are known to be unreliable for determining sufficient conditions for stability. For finite dimensional problems analysis of the spectrum can lead to sufficient conditions but in the PDE context, the size of the matrix becomes unbounded as the grid is refined. In our case the matrix is non-symmetric and non-normal, and for non-normal matrices, counterexamples can be given where, even if the eigenvalues are less than one in magnitude, instability results as the dimension of the matrix becomes large (see [11, 7, 9, 17]). For some values of the market parameters we are able to show that sufficient conditions for stability are satisfied using numerical range arguments [7, 8, 16, 3]. In other cases, these arguments cannot be applied and we follow [2] and

*This work was supported by the Natural Sciences and Engineering Research Council of Canada, the Social Sciences and Humanities Research Council of Canada and RBC Financial Group.

†Department of Computer Science, University of Waterloo, Waterloo ON, Canada N2L 3G1, hawindcliff@elora.math.uwaterloo.ca

‡Department of Computer Science, University of Waterloo, Waterloo ON, Canada N2L 3G1, paforsyt@elora.math.uwaterloo.ca,

§Centre for Advanced Studies in Finance, University of Waterloo, Waterloo ON, Canada N2L 3G1, kvetzal@watarts.uwaterloo.ca

demonstrate that the discrete timestepping operator is power-bounded, via numerical experiments.

2. Problem Formulation. We will consider the standard Black-Scholes equation, which can be written as:

$$V_t + (r-q)SV_S + \frac{\sigma^2 S^2}{2} V_{SS} - rV = 0 \quad , \tag{2.1}$$

where $V(S,t)$ represents the value of the derivative security, S is the value of the underlying security, r is the risk-free interest rate, q is the continuous dividend yield and σ, is the volatility of the underlying asset. In the following, we will make the simplifying assumptions that $\sigma = \sigma(S)$, and that r, q are constants, with $r > 0$. These assumptions are used to simplify some of the proofs which follow. In order to ensure that the stock price process is well-behaved, we assume that [13]

$$\begin{aligned} \sigma(S) &\leq C_1 \quad ; \quad S \to \infty \\ \frac{\partial (S^2\sigma^2)}{\partial S} &= 0 \quad ; \quad S \to 0 \ , \end{aligned} \tag{2.2}$$

where C_1 is independent of S. Once the contractually defined payoff of the derivative security, $V(S,T) = g(S)$, is specified, equation (2.1) can be solved backwards in time from the maturity date of the contract, $t = T$, to the present time, $t = 0$, in order to obtain the current value of the contract.

The original problem (2.1) is posed on the domain $[0, \infty)$. The boundary condition at $S = 0$ is obtained simply by setting $S = 0$ in equation (2.1). This results in the specification:

$$V_t(0,t) = rV \tag{2.3}$$

at the lower boundary. Of course, when using an implicit type of numerical scheme, we must truncate this domain to $[0, S_{max}]$. Consequently, it is also necessary to impose a boundary condition at $S = S_{max}$. If the error made in the approximation of this boundary condition is bounded then, by extending the computational domain, it is possible to make the near-field error (i.e. the error in the solution for practical values of S) arbitrarily small. In [6], detailed estimates are obtained for the error in the solution due to misspecification of the correct boundary condition at $S = S_{max}$. For example, in the case of a European call, with boundary condition at $S = S_{max}$ set to the payoff, and assuming that $\sigma^2 > 2r$, it is shown that if

$$S_{max} > K \exp(\sigma \mu \sqrt{T}) \tag{2.4}$$

where $\mu = \sqrt{2|\log(tol)|}$ and K is the strike, then the error in the solution at $S = K$ is less than $K \times tol$. In order to be able to utilize small computational domains, it is important that the error in the approximation of the boundary condition be as small as possible.

Equation (2.4) tends to be somewhat pessimistic. An alternative idea is based on the fact that the solution to the SDE

$$dS = S(r-q)\ dt + S\sigma\ dZ \tag{2.5}$$

where dZ is the increment of a Wiener process, is

$$S(T) = S_0 \exp\left((r - q - \frac{\sigma^2}{2})T + \sigma\phi\sqrt{T} \right) \ , \tag{2.6}$$

where ϕ is a random draw from a standard normal distributon with mean zero and unit variance. If we assume that the probability of $S(T)$ ocurring at μ standard deviations away from the mean is negligible, then this suggests that choosing an artificial boundary S_{max} such that

$$S_{max} > K \exp\left((r - q - \frac{\sigma^2}{2})T + \sigma\mu\sqrt{T} \right) , \tag{2.7}$$

should results in a small error near $S = K$. Typically, one chooses $\mu = 3$. Note that if we ignore the drift term in condition (2.7), then condition (2.7) is formally very similar to condition (2.4), but with a different criteria for selecting μ.

We note that in some circumstances, it may be desirable to specify a computational domain $[S_{min}, S_{max}], S_{min} > 0$, with artificial boundary conditions imposed at both S_{min}, S_{max}. In this paper, we will focus on the case where the computational domain is $[0, S_{max}]$, and we will point out the cases where the results can be extended to the case of a computational domain $[S_{min}, S_{max}], S_{min} > 0$.

For path-dependent options, estimates such as those given in [6] are not always sufficient to ensure accurate results. This is because the solution at points of interest may depend on far-field data (i.e. remote from S values of interest) through the contractually defined jump conditions. An example of such a situation is in the full three-dimensional numerical valuation of multiple shout options described in [22] where the required size of the computational domain grows exponentially with the number of shout opportunities. Some popular insurance products offered in Canada [21] can offer the investor as many as 60 total shout opportunities (referred to as "resets" in these contracts) over the life of the contract. Hence, for path-dependent products it can be extremely important to have an accurate method for approximating the boundary condition on the truncated computational domain.

2.1. Dirichlet Boundary Conditions. One of the simplest methods for specifying the boundary behavior is to provide a Dirichlet condition at S_{max}. In some cases, it is fairly straightforward to determine an asymptotic form of the PDE (2.1) using financial reasoning. The examples below demonstrate the ad hoc nature of the Dirichlet boundary specification:

$$\begin{aligned} \text{Call option:} \quad & V(S \to \infty, t) = Se^{-q(T-t)} \\ \text{Put option:} \quad & V(S \to \infty, t) = 0 \\ \text{Digital call option:} \quad & V(S \to \infty, t) = e^{-r(T-t)} \end{aligned}$$

The main difficulty with imposing a Dirichlet condition is that it is assumed that one has some additional knowledge about the behavior of the solution. In the simple examples given above, this asymptotic behavior can easily be determined. However, when modeling complex contracts the appropriate Dirichlet specification may not be obvious. As the examples above demonstrate, the Dirichlet condition is not suitable for general-purpose software designed for solving the Black-Scholes equation since the appropriate Dirichlet condition intimately depends upon the payoff of the derivative contract being priced, as well as assumptions about the stochastic process followed by the underlying asset. In addition, path-dependent options with jump conditions further complicate matters. Consequently, it is of much interest to find a way that automatically determines asymptotic behavior consistent with the financial context.

2.2. The Linear Boundary Condition. If the payoff is at most linear in S and if the stochastic process followed by the underlying asset is suitably well-behaved, then we can show that the value of the derivative security is asymptotically linear as $S \to \infty$. Path-dependent options also fit into this framework if the payoff is at most linear in the state variables and the jump conditions updating the state variables are at most linear. This includes simple call, put and digital options as well as Asian, lookback, barrier, shout and a host of other exotic options.

One way that we can implement this linear condition is to assume that V is of the form:

$$V(S,t) = a(t)S + b(t)$$

where the $a(t)$, $b(t)$ are to be determined. By substituting this form into (2.1) we obtain an ordinary differential equation (ODE) for the coefficients $a(t)$ and $b(t)$:

$$V_t(S \to \infty, t) = rb(t) + qa(t)S \ . \tag{2.8}$$

This separates into two ODEs and can be solved to obtain a time-dependent boundary specification that can be implemented using a Dirichlet node. In [21] we provide an example using this boundary specification for a very complex path-dependent option.

The ODE formulation offers a much simpler implementation compared with the Dirichlet node since the appropriate boundary condition is determined on the fly and does not need to be coded a priori for each class of contracts. However, for path-dependent options each new contract requires a different method for updating a and b after each jump condition. This is an error prone procedure and can lead to cumulative interpolation error.

An alternative is to impose the linear condition $V_{SS} = 0$ directly in the discretization of the PDE. With the assumption of linearity, the Black-Scholes equation becomes:

$$V_t + (r-q)SV_S - rV = 0 \ \ , \tag{2.9}$$

and the remaining spatial derivative, V_S, can be approximated using a one-sided finite difference using data in the computational domain. This approach has been suggested as a general technique by several authors including [18, 19, 10]. However, to our knowledge, there have been no detailed analyses of the stability properties of this method. In the typical situation where $r - q > 0$, this one-sided differencing can be thought of as using downstream weighting for the convective term. It is well known from the computational fluid dynamics (CFD) literature that downstream weighting often gives rise to numerical instability. As such, it is perhaps surprising that this method has been used for many years without reported difficulties.

It is also worth noting that this method has been re-invented many times in the literature. For example, in [10] the author derives the "natural boundary condition" in the finite element context. The natural boundary condition is formally equivalent to the linear boundary condition described in this paper.

2.3. The PDE Boundary Condition. Each of the methodologies given above for handling the boundary condition imposes some additional information; either a known value for the solution, or an assumption of linearity. In some situations, such as a power contract, whose payoff is given by $V(S,T) = S^p$ for some constant p, we are not able to assume the the value of the contract is asymptotically linear in S if

$p > 1$. Another example of a contract whose value is not asymptotically linear is a discretely observed variance swap.

In [18] the authors propose a boundary technique that does not require additional linearity assumptions. This FD method involves using one-sided derivatives for the spatial discretization of the PDE. In general, since we are not specifying any additional constraints on the behavior of the solution and downstream information is used for the convective terms, it is not obvious that this method will be stable.

3. Definitions of Stability. Equation (2.1) can be cast into the form of a convection-diffusion problem using the transformation $\tau = T - t$,

$$V_\tau = \frac{\sigma^2 S^2}{2} V_{SS} + (r - q) S V_S - rV \ . \tag{3.1}$$

Given a discrete grid of S-values, S_i, $i = 1, \ldots, n$, we represent the value of the derivative security, at time level $\tau = \tau_k$, by the vector V^k, where the i^{th} component is $V_i^k = V(S_i, \tau_k)$. A semi-discrete form of equation (3.1) can then be written as

$$V_\tau^k = -AV^k \tag{3.2}$$

where A is a discretization of the spatial operator in equation (3.1), i.e.

$$\begin{aligned} -AV^k = \frac{\sigma^2 S^2}{2} V_{SS}^k + (r - q) S V_S^k - rV^k \\ + \text{discretization error} \ . \end{aligned} \tag{3.3}$$

Now, if we discretize equation (3.2) in the time direction, we then obtain

$$(I + \theta A \Delta\tau) V^{k+1} = (I - (1 - \theta) A \Delta\tau) V^k \quad , \tag{3.4}$$

where $\theta = 0$ is fully explicit, $\theta = \frac{1}{2}$ is Crank-Nicolson and $\theta = 1$ is fully implicit timeweighting. To avoid algebraic complication, we will assume that any Dirichlet boundary conditions are time independent (it is straightforward to extend the analysis to the time-dependent case, at the expense of notational complexity). We can write the discrete equations (3.4) as

$$V^{k+1} = (I + \theta A \Delta\tau)^{-1} (I - (1 - \theta) A \Delta\tau) V^k \quad ,$$

or

$$V^{k+1} = BV^k \quad , \tag{3.5}$$

where the matrix B is defined[1] as

$$B = (I + \theta A \Delta\tau)^{-1} (I - (1 - \theta) A \Delta\tau) \quad . \tag{3.6}$$

If V^0 is the initial condition, then after k timesteps we have

$$V^k = B^k V^0 \quad . \tag{3.7}$$

[1] In Theorem 5.2 we will see that the eigenvalue of A, $\lambda = q$, is preserved and the remaining eigenvalues of A have non-negative real parts. As a result, it follows that the inverse of the matrix $(I + \theta A \Delta\tau)$ can always be computed if $q \geq 0$. If $q < 0$, then $(I + \theta A \Delta\tau)$ has a zero eigenvalue, and hence this matrix cannot be inverted when $\theta q \Delta\tau = -1$. However, this would require unrealistic values of q and $\Delta\tau$ and is not a problem of practical concern. Throughout this paper we impose the condition that $\Delta\tau < |1/q|$ when $q < 0$.

Given an arbitrary norm $\|\cdot\|$ we define the following notions of stability. We say that B is *strictly stable* if

$$\|B^k\| \leq 1,\ \forall k, n > 0\ . \tag{3.8}$$

Strict stability is also referred to as *practical stability* by some authors [14]. We also define *strong stability* as [5]

$$\|B^k\| \leq C,\ \forall k, n > 0\ , \tag{3.9}$$

and *algebraic stability* [5, 16] as

$$\|B^k\| \leq k^p n^l C,\ \forall k, n > 0\ , \tag{3.10}$$

where $C, p, l \geq 0$ are constants independent of k and n, where n is the dimension of B. The estimates (3.8), (3.9) and (3.10) must hold uniformly for the family of matrices generated by letting $\Delta S, \Delta\tau \to 0$, which implies that $n, k \to \infty$.

In this paper we are interested in studying the stability of the matrix operator B. If this operator is not stable, then small errors made during the numerical computations can be amplified, rendering the numerical solution useless. In particular, looking at the form of the discrete equations obtained using the linear boundary condition, we were initially very concerned that this method may lead to unstable discretizations. However, we will see that in usual situations this is not the case and that the linear boundary condition can be safely used in practice.

4. Form of the Discrete Equations. In this section we provide specific details concerning the FD discretization of the PDE at the interior nodes. The discretization discussed here utilizes upstream differencing when the governing equations become convection dominated. This ensures that the discrete equations corresponding to nodes in the interior of the domain are diagonally dominant.

The matrix A given in (3.4) is of the form:

$$A = \begin{bmatrix} r & 0 & & & & \\ -\alpha_2 & r+\alpha_2+\beta_2 & -\beta_2 & & & \\ & & & \ddots & & \\ & & & -\alpha_{n-1} & r+\alpha_{n-1}+\beta_{n-1} & -\beta_{n-1} \\ & & & \gamma_{n-2} & \gamma_{n-1} & \gamma_n \end{bmatrix}\ , \tag{4.1}$$

where the definitions of the coefficients $\gamma_{n-2}, \gamma_{n-1}$ and γ_n depend upon the boundary condition applied at S_{max}.

Letting $\sigma(S_i) \equiv \sigma_i$, then using a FD approach we can define:

$$\alpha_i = \frac{\sigma_i^2 S_i^2}{2D_i \Delta S_{i-1}} - \frac{(r-q)S_i}{2D_i} \tag{4.2}$$

$$\beta_i = \frac{\sigma_i^2 S_i^2}{2D_i \Delta S_i} + \frac{(r-q)S_i}{2D_i} \tag{4.3}$$

where $\Delta S_i = S_{i+1} - S_i$ and $D_i = (\Delta S_{i-1} + \Delta S_i)/2$. We will refer to a discretization which defines α_i and β_i according to (4.2-4.3) as a central-weighted FD scheme.

The use of central differencing for the convection term in (4.2-4.3) can lead to numerical artifacts when the governing equations become convection dominated. In

this situation, the discretization should switch to using upstream weighting for the convection terms. If $\alpha_i < 0$, the coefficients are defined as:

$$\alpha_i = \frac{\sigma_i^2 S_i^2}{2D_i \Delta S_{i-1}} \tag{4.4}$$

$$\beta_i = \frac{\sigma_i^2 S_i^2}{2D_i \Delta S_i} + \frac{(r-q)S_i}{\Delta S_i} \quad , \tag{4.5}$$

while if $\beta_i < 0$, then these coefficients are given by:

$$\alpha_i = \frac{\sigma_i^2 S_i^2}{2D_i \Delta S_{i-1}} - \frac{(r-q)S_i}{\Delta S_{i-1}} \tag{4.6}$$

$$\beta_i = \frac{\sigma_i^2 S_i^2}{2D_i \Delta S_i} \quad . \tag{4.7}$$

This ensures that $\alpha_i, \beta_i \geq 0$ and as a result, rows 1 through $n-1$ in matrix A are diagonally dominant. This central-upstream weighted FD discretization will be used predominantly throughout the paper unless we specify otherwise.

In the case of single-factor options, for typical values of σ and r we find that upstream differencing is only required at a small number of nodes, usually remote from the region of interest. Consequently use of this low order upstreaming scheme at a small number of nodes does not result in noticeably poor convergence as the grid is refined. However, for multi-factor options it is often desirable to use a high-order positive coefficient scheme [23]. We emphasize that in this paper our focus is on the specification of the boundary conditions, not the discretization at interior points, and we will not pursue these other discretization methods further in this work.

4.1. Discretization of the Boundary Condition. The spatial discretization given by (4.1) depends on γ_{n-2}, γ_{n-1} and γ_n, the discretization of the boundary condition imposed at S_{max}. We now specify how these coefficients are defined for a Dirichlet node, the linear condition and the PDE boundary condition.

Dirichlet Node Discretization. We can implement a Dirichlet node at the upper boundary of the domain by setting $\gamma_{n-2} = \gamma_{n-1} = \gamma_n = 0$ in matrix A, given by (4.1). (We remind the reader that we have assumed, for simplicity, that the Dirichlet boundary conditions are time independent).

Linear Condition Discretization. If we use fully implicit timeweighting and one-sided finite differences then equation (2.9) becomes:

$$\frac{V_n^{k+1} - V_n^k}{\Delta\tau} = (r-q)S_n \left(\frac{V_n^{k+1} - V_{n-1}^{k+1}}{\Delta S_{n-1}} \right) - rV_n^{k+1} \quad . \tag{4.8}$$

This boundary specification can be represented by choosing:

$$\gamma_{n-2} = 0 \tag{4.9}$$

$$\gamma_{n-1} = \frac{(r-q)S_n}{\Delta S_{n-1}} \tag{4.10}$$

$$\gamma_n = r - \gamma_{n-1} \ . \tag{4.11}$$

Looking at these coefficients we see that with the linear boundary condition the discrete spatial operator, represented by the matrix A, is not guaranteed to be diagonally dominant when $r - q > 0$, which is a realistic situation for the parameters r and q.

Note that if A has properties $diag(A) > 0$, $offdiag(A) \leq 0$, and $rowsum(A) \geq 0$, then $I + \Delta\tau A$ is an M matrix. If $I + \Delta\tau A$ is an M matrix then $(I + \Delta\tau A)^{-1} \geq 0$, and hence it is straightforward to show that a fully implicit discretization is unconditionally stable.

The PDE Boundary Discretization. In [18] the authors propose a technique that does not require any additional assumptions. This finite difference method involves using one-sided derivatives for the spatial discretization of (3.1). We can implement this technique at the upper boundary by choosing:

$$\gamma_{n-2} = -\frac{\sigma_i^2 S_n^2}{\Delta S_{n-2}(\Delta S_{n-1} + \Delta S_{n-2})} \tag{4.12}$$

$$\gamma_{n-1} = \frac{\sigma_i^2 S_n^2}{\Delta S_{n-1}\Delta S_{n-2}} + \frac{(r-q)S_n}{\Delta S_{n-1}} \tag{4.13}$$

$$\gamma_n = r - \gamma_{n-1} - \gamma_{n-2} \quad . \tag{4.14}$$

We can see that when $\sigma = 0$, this method is equivalent to the linear boundary condition described in the previous section, obtained by imposing $V_{SS} = 0$ at the boundary.

5. Necessary Conditions for Stability. Recall that the semi-discrete representation of the differential equation (3.1) is given by

$$\frac{\partial}{\partial\tau}V^k = -AV^k \ , \tag{5.1}$$

where A is defined according to (4.1). The matrix A represents the discretization of the spatial operator:[2]

$$\mathcal{L}(V) = -\frac{\sigma^2 S^2}{2}V_{SS} - (r-q)SV_S + rV \quad . \tag{5.2}$$

By direct substitution, we see that $\mathcal{L}(S) = qS$, implying that $\lambda = q$ is an eigenvalue of this spatial operator corresponding to the eigenvector $V = S$. We remind the reader that we are assuming that $r > 0$. If $q < 0$, the operator $\mathcal{L}$ has a negative eigenvalue and hence the partial differential equation (3.1) has an exponential growth.[3] On the other hand, if $q \geq 0$, then it can be shown that all of the eigenvalues of the spatial operator $\mathcal{L}$ are real and non-negative. It would seem appropriate to attempt to enforce these properties in the discrete spatial operator, A, as well. We define a legitimate discretization of the spatial operator as follows:

DEFINITION 5.1. *A legitimate discretization of the spatial operator (5.2) has the properties that if $\{\lambda_i\}$ are the eigenvalues of the matrix A given by equation (4.1) then:*

1. *Case $q \geq 0$: All of the eigenvalues must satisfy $Re(\lambda_i) \geq 0$.*
2. *Case $q < 0$: There is at most a single index ρ for which $Re(\lambda_\rho) < 0$.*

REMARK 5.1. *A legitimate discretization has the satisfying property that the discrete spatial operator preserves certain spectral properties of the continuous spatial operator.*

[2]The matrix A was defined to be the negative of the usual spatial operator in order to simplify certain proofs concerning the properties of the spectrum of this matrix.

[3]Although the dividend yield is never negative, setting $q < 0$ may be used to model the cost of carry when pricing an option where the underlying is a commodity. Similar situations can arise when valuing real options (see, e.g. [4]), although the parameters are interpreted in a different context.

In Section 5.1 we prove that the linear boundary condition, used in conjunction with the FD discretization given above, yields a legitimate discretization. However, we are really interested in the stability of the discrete matrix operator B. The necessary conditions for stability are closely related to the concept of legitimacy of the spatial discretization.

Let the eigenvalues of B be denoted by $\{\Lambda_i\}$. We can relate the eigenvalues of B with the eigenvalues of A for specific timeweightings. If λ_i is an eigenvalue of the matrix A, then the corresponding eigenvalue of B for a fully implicit timestepping strategy ($\theta = 1$) is given by

$$\Lambda_i = \frac{1}{1 + \lambda_i \Delta\tau} \quad . \tag{5.3}$$

For a Crank-Nicolson timestepping strategy ($\theta = \frac{1}{2}$), the corresponding eigenvalue of B is given by

$$\Lambda_i = \frac{1 - \frac{\lambda_i \Delta\tau}{2}}{1 + \frac{\lambda_i \Delta\tau}{2}} \quad . \tag{5.4}$$

In the remainder of this paper we will consider only fully implicit and Crank-Nicolson timeweightings.

Strict stability of the timestepping method (3.7) implies that the following necessary conditions must be satisfied [14]:

- $|\Lambda_i| \leq 1$, $\forall i$,
- If there is an eigenvalue such that $|\Lambda_i| = 1$ then, in order to avoid algebraic growth, the algebraic and geometric multiplicities of this eigenvalue must be the same.

We will find that the legitimacy of the spatial discretization will be directly related to the necessary conditions for stability of the timestepping algorithm.

5.1. Legitimacy of the Linear Boundary Condition. We now show that the FD spatial discretization (4.2-4.7) using the linear boundary condition (4.9-4.11) is legitimate.

THEOREM 5.2. *Let $r \geq 0$ and suppose that the matrix coefficients α_i, β_i are given by (4.2-4.7) and the boundary coefficients γ_i are given by (4.9-4.11). If matrix A represents the spatial discretization given in (4.1) then the discretization preserves the eigenvalue $\lambda = q$ and the remaining eigenvalues have a non-negative real part.*

Proof. We begin by showing that this discretization preserves the eigenvalue $\lambda = q$. By direct substitution, we see that if $V = (S_1, S_2, \ldots S_n)^T$, then $AV = qV$. Thus q is an eigenvalue of the matrix A.

We define the parameterized matrix

$$A(h) = D + (A - D)h \qquad \text{for } h \in [0, 1]$$

where $D = \text{diag}(A)$. As $A(0) = D$ and $A(1) = A$, the eigenvalues of $A(h)$ trace continuous curves[4] that join the diagonal entries to the eigenvalues of A. We let $\lambda_i(h)$ represent the path traced by the eigenvalue starting at the diagonal entry a_{ii}. We can

[4]See [1] for a proof that the eigenvalues of a matrix whose coefficients are parameterized over a real interval are continuous functions.

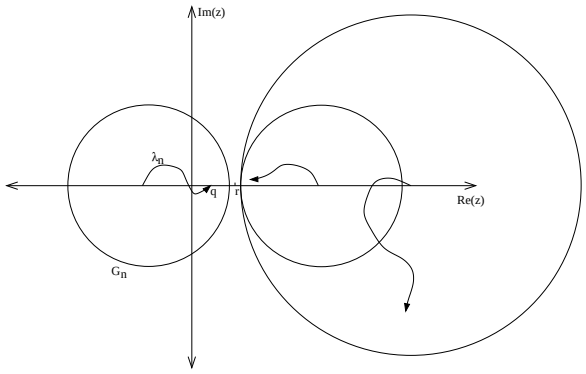

FIG. 5.1. *A snapshot of some of the Gerschgorin disks and the conceptual paths traced by some of the eigenvalues for some $h < 1$ in the case where $r - q > 0$. The disk $G_n(h)$ is disjoint from the remaining disks for $h < 1$. We show that the final location of the only eigenvalue which is contained in the interior of this disk is given by $\lambda_n(1) = q$.*

build a parameterized family of Gerschgorin disks for $A(h)$ given by

$$\begin{aligned} G_1(h) &= \{r\} \\ G_i(h) &= \{z \in \mathbb{C} : |z - (r + \alpha_i + \beta_i)| \leq (\alpha_i + \beta_i)h\} \qquad \text{for } i = 2, \ldots, n-1 \\ G_n(h) &= \{z \in \mathbb{C} : |z - (r - \gamma_{n-1})| \leq |\gamma_{n-1}|h\} \quad , \end{aligned}$$

as depicted in Figure 5.1. We remind the reader that the Gerschgorin Circle Theorem states that each eigenvalue of A is contained in at least one of the Gerschgorin disks $G_i(1)$, and in the union of these disks, each connected region contains at least one eigenvalue. Since $\alpha_i, \beta_i \geq 0$, we see that each of the disks $G_i(h)$, for $i = 1, \ldots, n-1$ only contain points satisfying $Re(z) \geq r \geq 0$ for all $h \in [0, 1]$. We now investigate the n^{th} disk in several special cases.

Case $r - q \leq 0$: In this case, $G_n(h)$ contains only points satisfying $Re(z) \geq r$. Since the eigenvalues of A must lie in the union of the Gerschgorin disks when $h = 1$, we have $Re(\lambda) \geq r \geq 0$ and the proof is complete.

Case $r - q > 0$: If we consider $\lambda_i(h)$ for any $i = 1, \ldots, n-1$, then $Re(\lambda_i(h)) \geq r$ for all $h \in [0, 1)$. To see this, we note that

$$\lambda_i(h) \in \bigcup_{k=1}^{n-1} G_k(h) \quad \forall\, h \in [0, 1),\ i = 1, \ldots, n-1$$

where we have used the fact that $G_n(h)$ is disjoint from the remaining disks if $0 \leq h < 1$. Suppose that $Re(\lambda_i(1)) = r - \epsilon$ for some $\epsilon > 0$. This contradicts the fact that $\lambda_i(h)$ is a continuous function of h and hence we can conclude that $Re(\lambda_i(1)) \geq r \geq 0$ for all $i = 1, \ldots, n-1$. As a result, the only eigenvalue of the matrix A which could possibly have a negative real part would be $\lambda_n(1)$. We notice that q is contained in the interior of the disk $G_n(1)$, so $\lambda_n(1) = q$. Therefore, the eigenvalue $\lambda = q$ is preserved by the discretization and all the remaining eigenvalues have non-negative real parts as they are bounded by $Re(\lambda) \geq r \geq 0$. □

COROLLARY 5.3. *Under the conditions outlined in the statement of Theorem 5.2 the spatial discretization, A, is legitimate.*

We now relate the concept of legitimacy with necessary conditions for stability of the discrete equations.

THEOREM 5.4. *A legitimate FD discretization using the linear boundary condition satisfies necessary conditions for stability for fully implicit and Crank-Nicolson timeweightings provided $r > 0$ and provided that when $q < 0$ the timestep restriction $\Delta\tau < |1/q|$ is satisfied.*

Proof. If we consider the case where $q \geq 0$, a legitimate discretization has $Re(\lambda_i) \geq 0$, and consequently $|\Lambda_i| \leq 1$. An eigenvalue where $|\Lambda_i| = 1$ occurs when there is an eigenvalue of A given by $\lambda_i = 0$. In the proof of Theorem 5.2 we saw that the FD discretization obtained in conjunction with the linear boundary condition has at most a single eigenvalue such that $Re(\lambda_i) < r$. Consequently, if $r > 0$ the matrix B can have at most a single eigenvalue where $|\Lambda_i| = 1$, which implies that the algebraic and geometric multiplicities of this eigenvalue must be the same. As a result, when $r > 0$ we see that legitimate discretizations of the spatial operator lead to fully implicit and Crank-Nicolson timestepping algorithms that satisfy necessary conditions for strict stability when $q \geq 0$.

In the case when $q < 0$, the partial differential equation has an exponentially growing mode, corresponding to $V = S$. In this case, according to Definition 5.1, a legitimate discretization allows a single eigenvalue of A to have $Re(\lambda_\rho) < 0$ and this eigenvalue is given by $\lambda_\rho = q$. Assuming $\Delta\tau < \frac{1}{|\lambda_\rho|}$, the matrix B will be invertible (see footnote (1)) and (5.3) and (5.4) will admit a series expansion for this eigenvalue. From the series expansion we see that legitimate discretizations allow a single eigenvalue of B to have the form:

$$|\Lambda_\rho| = 1 + C\Delta\tau \ ,$$

for some constant C which is independent of $\Delta\tau$ and ΔS. This is consistent with necessary conditions for a weaker form of stability given in [14], which allows exponentially growing modes but requires that they remain bounded for any fixed time horizon as $\Delta\tau \to 0$.

Assuming $r > 0$, the remaining eigenvalues satisfy $|\Lambda_i| < 1$, $\forall i \neq \rho$. Hence, when $q < 0$, legitimate discretizations of the spatial operator lead to fully implicit and Crank-Nicolson timestepping algorithms that satisfy necessary conditions for stability consistent with the behavior of the governing differential equations. □

The assumption that r is strictly positive appears to be a technical limitation of the proof given above. In practice, even when $r = 0$ we do not observe algebraic growth in the discrete solution.

REMARK 5.2. *Note that a legitimate discretization satisfies the necessary conditions for stability. However, a non-legitimate discretization may also satisfy necessary conditions for stability. For example, consider a case where $q > 0$. In this case, suppose we have a non-legitimate discretization, where there is an eigenvalue $|\Lambda_\rho| = 1 + C\Delta\tau$ (where C is independent of $\Delta\tau$ and ΔS). This discretization would be stable, but the spectrum would be inconsistent with the spectrum of the continuous PDE.*

REMARK 5.3. *If the boundary condition $V_{SS} = 0$ is also applied at $S = S_{min}$, and one sided differencing is used for the V_S term at $S = S_{min}$, then the above arguments can be easily (although tediously) extended to show that Theorem 5.4 applies to this case as well.*

5.2. Non-Legitimacy of the PDE Boundary Condition. In the previous section we showed that the linear boundary condition results in a legitimate discretiza-

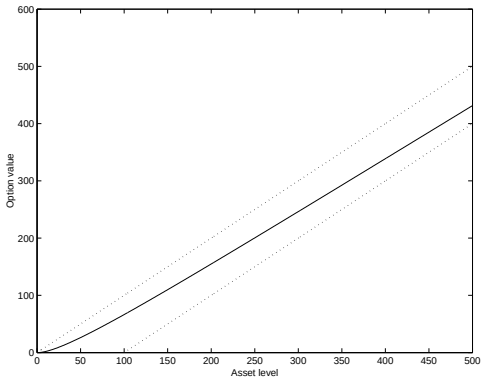

(a) *Linear Boundary Condition*

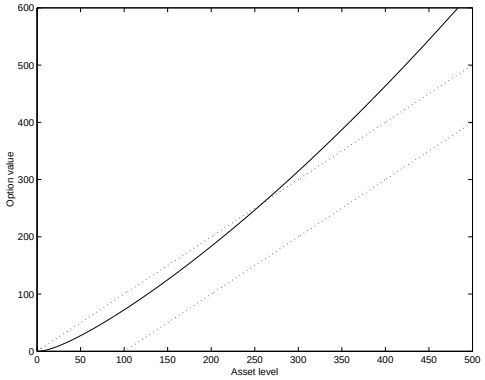

(b) *PDE Boundary Condition*

FIG. 5.2. *Demonstration of inconsistent exponential growth for the PDE Boundary Condition. When there are no dividends, the solution is known to be bounded by* $S - K \leq V \leq S$ *as given by the dotted lines. The contract is a European call option with* $K = \$100$, $T = 10$ *years,* $\sigma = 50\%$, $r = 5\%$ *and* $q = 0\%$. *The numerical computations used a 50 node asset price grid with constant spacing and* $S_{max} = \$500$. *A fully implicit time-weighting was used with constant timesteps of size* $\Delta\tau = .01$ *years.*

tion and hence satisfies necessary conditions for stability. That is not the case for the PDE boundary condition. Experimentally we observe that, even when $q \geq 0$, the matrix A representing the spatial discretization can have negative eigenvalues when using the PDE boundary condition. To demonstrate that this method can introduce exponential growth that is inconsistent with the governing equations, we consider a long-term, $T = 10$ year, European call option on a relatively volatile stock with $\sigma = 50\%$. For this example, we use constant grid spacing and fully implicit time weighting with constant timesteps.

In Figure 5.2 the inconsistent exponential growth described above is clearly visible. When there are no dividends, the solution is known to lie between $S - K \leq V \leq S$, as given by the dotted lines. We see that these bounds are satisfied in Figure 5.2(a) when the linear boundary condition is imposed. In Figure 5.2(b) the PDE boundary condition is used and the solution has drifted substantially outside of these known bounds. In this example, we experimentally observe that the matrix A has a negative eigenvalue given approximately by $\lambda \simeq -.2209$, and hence the necessary condition for strict stability is violated. However, it is possible that the PDE boundary condition

	Boundary Specification			
	ODE	Linear BC	PDE BC	Analytic
Refinement level	Value at $S = \$100$ ($)			
1	66.42	66.41	72.62	67.32
2	67.26	67.25	67.54	↓
3	67.31	67.31	67.32	
4	67.32	67.32	67.32	

TABLE 5.1

Effect of imposing various artificial boundaries on the numerical solution of long maturity European call option with $K = \$100$, $T = 10$ years, $\sigma = 50\%$, $r = 5\%$ and $q = 0\%$. The numerical computations were performed on a grid with constant spacing with endpoints $[0, S_{max}]$ using a fully implicit timeweighting with constant timesteps. The first refinement level used: $\Delta\tau = .01$ years $S_{max} = \$500$, and had 50 asset price nodes. Subsequent refinement levels doubled S_{max} as well as reducing the timestep size and grid spacing by factors of two. The ODE boundary condition is given by (2.8).

could still be strongly stable, since legitimacy is a stronger condition than stability.

We see in Table 5.1 that the quality of the solution obtained near the exercise price, $S = \$100$, has also degraded when using the PDE boundary condition for the first few refinement levels; i.e. when S_{max} is small. This is a relatively extreme example, with high volatility and a very long maturity. In fact, if we estimate S_{max} using equation (2.7), assuming that a three standard deviation event is negligible, then this suggests that $S_{max} \simeq 5000$. Table 5.1 indicates that all methods get four figure accuracy with $S_{max} = 4000$.

Note that we have used a very small S_{max} on the coarse grid in Table 5.1. One should view these tests as carried out with somewhat extreme parameters. For typical parameters it is often very difficult to detect problems when only looking at the computed solution. From Table 5.1, it appears that the effect of the negative eigenvalue in A is small (at S values of interest) if S_{max} is sufficiently large. However, we do recommend that care be taken when using the PDE boundary condition.

6. Sufficient Conditions for Stability. As mentioned above, requiring that the eigenvalues have magnitude less than one is a necessary condition for stability. The spectrum of the evolution matrix can lead to unreliable stability estimates in the PDE context where the size of the matrix grows as the grid is refined. Because of the structure of the spatial matrix when the linear boundary condition is applied, numerical range, energy methods and von Neumann analysis do not appear to be applicable to this problem. Consequently, we must investigate the power-boundedness of the matrix B. In the following, we use the maximum norm, $\|\cdot\| = \|\cdot\|_\infty$, where:

$$\|v\|_\infty = \max_i |v_i|, \; \forall v \in \mathbb{R}^n \; ,$$

and the associated induced matrix norm is:

$$\|B\|_\infty = \max_{v \in \mathbb{R}^n} \frac{\|Bv\|_\infty}{\|v\|_\infty} = \max_i \sum_j |b_{ij}| \; .$$

We will use the notation B_n^k to refer to the matrix B, of dimension n, raised to the k^{th} power.

We should point out that there are two tests of stability. One involves taking a large number of timesteps of fixed size while the other involves keeping a fixed time

		k					
		1	10	50	100	250	1000
Timestep type	n	$\|B_n^k\|_\infty$					
Fully implicit	$\forall n$	1.00	1.00	1.00	1.00	1.00	1.00
Crank Nicolson	51	2.42	1.63	1.00	1.00	1.00	1.00
	101	2.70	2.19	1.34	1.00	1.00	1.00
	201	2.85	2.52	1.96	1.55	1.05	1.00
	401	2.92	2.70	2.33	2.06	1.71	1.05
	801	2.95	2.79	2.53	2.33	2.12	1.71
	1601	2.97	2.83	2.63	2.48	2.34	2.12

TABLE 6.1

Power-boundedness of B using a Dirichlet node. The table gives $\|B_n^k\|_\infty$, where B is defined according to (3.6) and n is the dimension of the matrix. The parameters used for this example are $r = .1$, $q = 0$, $\sigma = .2$, $\Delta\tau = .1$. The grid used variable spacing and $S_{max} = \$250$.

horizon and reducing the timestep size, thereby also taking an unbounded number of timesteps. In the following we present results for computations using an unbounded number of fixed size timesteps, for the $V_{SS} = 0$ boundary condition. We also ran numerical experiments where the timestep size was reduced and the time horizon was kept fixed. For brevity, we only present the fixed timestep results. The results for a fixed time horizon lead to the same conclusions.

Sufficient conditions for stability using a Dirichlet node. If a time independent Dirichlet node is specified with fully implicit timestepping, then the matrix A in equation (3.4) has the last row identically zero. Further, if $\alpha_i, \beta_i \geq 0$, in equation (4.1), then $(I + A\Delta\tau)$ is an M-matrix, hence it is straightforward to show, using maximum principles [12], that $\|V^{k+1}\|_\infty \leq \|V^k\|_\infty$, and hence strict stability follows, with no restrictions on the timestep size. If a Dirichlet node value $V(S_{max}) = V_d(t)$ is time dependent, then the stability result is $\|V^{k+1}\|_\infty \leq \max(\|V^k\|_\infty, |V_d^{k+1}|)$.

In Table 6.1 we provide a demonstration of power-boundedness for the matrix B given by (3.6) obtained using a Dirichlet boundary condition. When fully implicit timestepping is used, we have proven that the discretization is strictly stable and we can see that this is consistent with the results in Table 6.1 where $\forall n, k > 0$, $\|B_n^k\|_\infty = 1$.

Using Crank-Nicolson timestepping, we no longer have an M-matrix and we cannot use maximum analysis to guarantee stability. Using a Dirichlet node, the convex hull of the Gerschgorin disks of A lies in the right half plane. From [8] this allows us to guarantee algebraic stability in the sense that:

$$\|V^k\|_\infty \leq Ck^{1/2}\|V^0\|_\infty \qquad \text{for } n, k > 0 \tag{6.1}$$

where n is the number of nodes in the asset price grid, k is the number of timesteps taken and where C is a constant independent of n, k, and V^0. This result holds with no restrictions on the timestep size $\Delta\tau$, and for non-constant coefficients. Note that the usual von Neumann analysis can only be applied if the PDE coefficients are constants.

Although we are able to guarantee the weaker stability estimate (6.1) using numerical range arguments [8], our numerical experiments indicate that the algebraic growth, $k^{1/2}$, does not occur in practice. If we scan across the rows of Table 6.1 we see that as $k \to \infty$, $\|B_n^k\|_\infty$ decays. As a result, the largest values of $\|B_n^k\|_\infty$ occur in

the left-most column, corresponding to $k = 1$. Scanning down the first column, as n increases the maximum size of $\|B_n^k\|_\infty$ appears to be converging to a number around 3. This indicates that $\|B_n^k\|_\infty$ is bounded above by a constant that is independent of k. Hence, we experimentally observe that the Dirichlet boundary specification results in strong stability when Crank-Nicolson timeweighting is used, although using numerical range arguments we were only able to guarantee algebraic stability. This subtle distinction is important since the Lax Equivalence Theorem states that, for linear problems, strong stability is a sufficient and necessary condition for the convergence of a consistent discretization for all initial data. For a discussion on the relationship of algebraic stability to the usual notions of stability and convergence see [5].

Stability using the linear boundary condition. When the linear boundary condition is applied and $r - q \leq 0$, the Gerschgorin disks of A all lie to the right of $z = r$ in the complex plane. Again calling on the numerical range results in [8] we can show that the discrete operator B is guaranteed to be algebraically stable. The case $r - q = 0$ holds for options on futures contracts and $r - q < 0$ can occur in FX options, where r and q represent the risk-free rates in the two currencies. Recall that this situation corresponds to an outflow boundary condition as $S \to \infty$ and the proper upstream weighting is used for the convection term in this case.

In the situation where $r - q > 0$, when the linear boundary condition is applied the numerical range arguments are not directly applicable. Looking at Figure 5.1, we see that not all of the Gerschgorin disks lie in the stability region. Even if we collapse these disks towards the convex hull of the spectrum, we require q to be positive and bounded away from zero in order not to include any points with negative real part. As a result, numerical range stability region arguments [8, 16] cannot be directly applied to this problem to guarantee stability in the typical case when $q = 0$. As mentioned previously, determination of sufficient conditions for stability in the case where the discrete equations have non-constant coefficients, along with non-standard boundary conditions, is a difficult task. In [15, 16], numerical methods were used to show stability for a range of input parameters. We will follow a similar approach here, and provide a numerical demonstration that the matrix B is strongly stable for a variety of input parameters.

In Table 6.2 we provide a demonstration of stability for the matrix B given by (3.6) when the linear boundary condition is applied. The results are quite similar for both fully implicit and Crank Nicolson timeweighting. Scanning across the rows of this table we see that for a fixed dimension n, $\|B_n^k\|_\infty$ is bounded as number of timesteps increases. Scanning down the last column, we see that the power-bound appears to be converging to some number slightly larger than 12 as the dimension of the matrix increases. Since this constant is reasonably small, errors introduced during the computations will not be amplified enough to noticeably affect the numerical solution.

Variations in the market parameters. The numerical experiments given in Table 6.1 and Table 6.2 provide a demonstration for a particular choice of market parameters r, q and σ with a given fixed $\Delta\tau$ and grid spacing. We have performed numerous other experiments, with different grid spacings and different timestep sizes, and all have indicated that the family of matrices B generated by this discretization using the linear boundary condition is power-bounded by a constant. To investigate the effects of the parameters r and σ, in Figure 6.1 we plot the experimental bound for $\|B_n^k\|_\infty$, $n, k > 0$ as a function of r and σ. This experimental bound was obtained by refining the grid, and thereby increasing the dimension n of the matrix, and increasing

		k					
		100	200	400	800	1600	3200
Timestep type	n	$\|B_n^k\|_\infty$					
Fully implicit	51	6.73	8.45	9.31	9.45	9.45	9.45
	101	7.60	9.52	10.47	10.62	10.63	10.63
	201	8.09	10.12	11.12	11.28	11.28	11.28
	401	8.35	10.43	11.47	11.63	11.63	11.63
	801	8.49	10.60	11.65	11.81	11.81	11.81
	1601	8.56	10.68	11.74	11.90	11.91	11.91
Crank Nicolson	51	6.75	8.47	9.32	9.45	9.45	9.45
	101	7.62	9.53	10.48	10.62	10.63	10.63
	201	8.11	10.13	11.13	11.28	11.28	11.28
	401	8.37	10.45	11.47	11.63	11.63	11.63
	801	8.51	10.61	11.65	11.81	11.81	11.81
	1601	9.05	10.83	11.74	11.90	11.91	11.91

TABLE 6.2

Power-boundedness of B using the linear boundary condition. The table gives $\|B_n^k\|_\infty$, where B is defined according to (3.6) and n is the dimension of the matrix. The parameters used for this example are $r = .1$, $q = 0$, $\sigma = .2$, $\Delta\tau = .1$. The grid used variable spacing and $S_{max} = \$250$.

n	401	801	1601	3201
$\|B_n^k\|_\infty,\ k > 0$	160	320	640	1280

TABLE 6.3

Unbounded growth in $\|B_n^k\|_\infty$, $k > 0$ as the dimension of the matrix $n \to \infty$ when $\sigma = 0$ using the linear boundary condition. Other parameters used for this example are $r = .10$, $q = 0$. $\Delta\tau = .1$ Fully implicit timestepping was used and the grid used variable spacing with $S_{max} = \$250$.

k until the computed value of $\|B_n^k\|_\infty$ was unchanged to a precision that could not be observed in the graph.

In Figure 6.1(a) we see that the power-bound on B is well-behaved and relatively unaffected by (r, σ) when σ is sufficiently large. However, $\|B_n^k\|_\infty$ increases rapidly for small volatilities as σ tends to zero. For a small fixed (but non-zero) σ we would expect that imposing the condition $V_{SS} = 0$ at a finite S_{max} would induce less error as we increase the size of the computational domain $[0, S_{max}]$. In Figure 6.1(b) we have increased the computational domain so that S_{max} is now \$1000. We find $\|B_n^k\|_\infty$ is less than that obtained with the smaller computational domain given in Figure 6.1(a) where $S_{max} = \$250$. This indicates that the stability behavior for small σ improves as the size of the computational domain increases.

In the special case when $\sigma = 0$ we observe in Table 6.3 that the power-bound continues to grow with the dimension of the matrix n. From Table 6.3, it appears that for $\sigma = 0$, $\|B_n^k\|_\infty \leq nC$ where C is independent of k and n. This indicates that for the special case $\sigma = 0$, the discrete operator B is only algebraically stable.

However, in numerical experiments performed when $\sigma = 0$ we did not notice instability in the actual numerical solution. Although round-off errors could excite these modes, for a fixed mesh size the amplification of these errors is bounded. The matrices given in Table 6.3 are larger than those which would arise in practical applications. In fact, the grid spacing near $S = \$100$ is approximately one cent for the grid with 3200 nodes. For these large matrices, the power-bound obtained when $\sigma = 0$ is

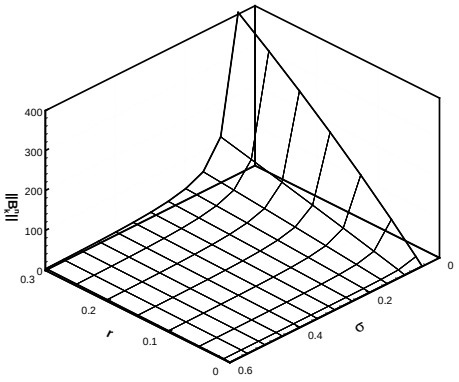

(a) $S_{max} = \$250$

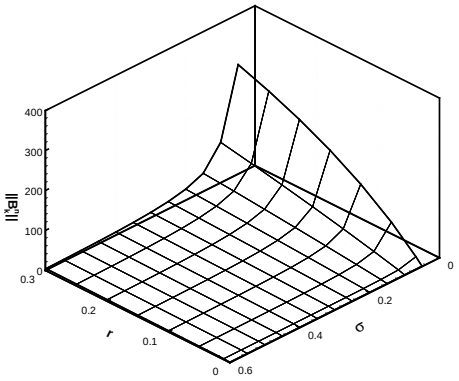

(b) $S_{max} = \$1000$

FIG. 6.1. *Power-boundedness of B as a function of r, σ. The plot gives C such that $\forall n, k > 0$, $\|B_n^k\|_\infty \leq C$ where B is defined according to (3.6) and n is the dimension of the matrix. Other parameters used for this example are $q = 0$ and $\Delta\tau = .1$. Fully implicit timestepping was used and the grid used variable spacing.*

roughly 10^3, indicating that errors may be amplified by approximately three orders of magnitude. To explain why this growth does not become evident in practice, we look at the lower right hand corner of the matrix B_n^k, where $n = 401$ and $k = 10000$:

$$B_{401}^{10000} = \begin{bmatrix} 0 & \dots & 0 & 0 & \vdots & \vdots \\ \vdots & \ddots & \vdots & \vdots & \vdots & \vdots \\ 0 & \dots & 0 & 0 & \text{-76.00} & 76.00 \\ 0 & \dots & 0 & 0 & \text{-77.00} & 77.00 \\ 0 & \dots & 0 & 0 & \text{-78.00} & 78.00 \\ 0 & \dots & 0 & 0 & \text{-79.00} & 79.00 \\ 0 & \dots & 0 & 0 & \text{-80.00} & 80.00 \end{bmatrix}$$

The matrix is of this form because when $\sigma = 0$ we are essentially solving a convection problem and after a large number of timesteps the solution depends only on the data at the inflow boundary.

The matrix shown above was used to estimate $\|B_n^k\|_\infty$, $k > 0$ in Table 6.3 when $n = 401$. For this matrix, the maximum norm is 160, which was obtained by summing the absolute values of the entries in the last row. To maximally excite this mode requires an initial condition of the form

$$V^0 = (0,\ 0,\ 0,\ 0,\ 0,\ \cdots,\ -1,\ 1)^T\ ,$$

which would not occur in reasonable financial applications. In applications, since the contractual payoff, $V(S,T)$, is nicely behaved and is discretized to generate the initial condition, V^0, typically the quantity $|V_n^0 - V_{n-1}^0|$ would be small.

In fact, in practice $V(S,T)$ is usually asymptotically linear. In this important special case, we see that $|V_n^0 - V_{n-1}^0|$ decreases linearly as the grid is refined. Our numerical experiments in Table 6.3 indicate that the bounding constant grows linearly as the grid is refined. These effects offset each other, explaining why the instability is not observed in practice. This is consistent with the conclusions of the Lax Equivalence Theorem which proves that strong stability is necessary and sufficient for convergence for *all* initial data. Weaker algebraic stability yields convergence only for *certain* initial data. For a further discussion of these results, see [5].

Although we have explored the case $\sigma = 0$ in some detail, it should be noted that in practice, $\sigma \geq \sigma_0 > 0$. The case $\sigma = 0$ represents a situation where there is no random component in the underlying stochastic process, which implies that the financial asset evolves with no uncertainty. For the practical case where $\sigma \geq \sigma_0 > 0$, the numerical results indicate that the discretization with a linear boundary condition at $S \to \infty$ is strongly stable. However, an interesting avenue for future research is to investigate the stability of the linear boundary condition in higher dimensional problems. For example, stochastic volatility models will include the case $\sigma = 0$ in the computational domain.

Power bound for the PDE boundary condition. As a final test, it is interesting to examine the power bound of B (equation (3.6) for the PDE boundary condition. For a fixed timestep size, for some choices of model parameters, $\|B_n^k\|_\infty$ becomes exponentially unbounded as $k \to \infty$ (see example in Section 5.2), since this discretization does not satisfy the necessary conditions for a legitimate discretization. However, it would appear from Table 5.1 that the PDE method does seem to give reasonable solutions if the computational domain is sufficiently large, and the timestep size is small. Table 6.4 shows the experimental results for $\|B_n^k\|_\infty$ for a sequence of tests. On each test, the expiry time is fixed, and the grid spacing and timestep size is halved on each refinement. To keep this consistent with our previous tests, we fix $S_{max} = 5000$ for all refinements. According to criteria (2.7) with $m = 3$, $S_{max} \simeq 5000$ is a reasonable choice. These tests are then similar to the tests shown in in Table 5.1, except that we keep S_{max} fixed. Table 6.4 shows with that for this refinement procedure, $\|B_n^k\|_\infty$ becomes unbounded as $n, k \to \infty$ for the PDE boundary condition. Hence the PDE boundary condition method is not stable, even for weak stability conditions [14]. However, Table 6.4 does indicate that the PDE boundary condition method is algebraically stable (linear growth in the power bound), if we carry out a grid refinement for fixed T. Table 5.1 shows that this unbounded growth in $\|B_n^k\|_\infty$ does not produce poor results, at least near the strike. Consequently, it would seem that for practical grid sizes and timesteps, the effect of the amplification of round off errors may be small.

	Expiry Time	
Refinement Level	5 years	10 years
1	4525	17167
2	9025	34224
3	18024	68336

TABLE 6.4

$\|B_n^k\|_\infty$ for the PDE boundary condition. Long maturity European call option with $T = 10$, $K = \$100$, $\sigma = 50\%$, $r = 5\%$ and $q = 0\%$. The numerical computations were performed on a grid with constant spacing with endpoints $[0, S_{max}]$ using a fully implicit timeweighting with constant timesteps. The first refinement level used: $\Delta\tau = .01$ years $S_{max} = \$5,000$, and had 500 asset price nodes. Subsequent refinement levels reduced the timestep size and grid spacing by factors of two, while keeping S_{max} fixed.

7. Extension of Results to Other Option Pricing PDEs. If the transformation $X = \log S$ is used, then PDE (2.1) becomes

$$V_\tau = \frac{\sigma^2}{2} V_{XX} + (r - q - \frac{\sigma^2}{2}) V_X - rV \ . \tag{7.1}$$

In this case, if we use the computational domain $[X_{min}, X_{max}]$, then the condition $V_{SS} = 0$ becomes $V_X = V_{XX}$ at $X = X_{min}, X_{max}$. Note that in this case, e^X is an eigenfunction of the continuous spatial operator, but not of the usual finite difference discretization of equation (7.1). This contrasts to the case where if the equation is discretized in the S coordinates, then $V = S$ is an eigenfunction of both the continuous and discrete operators. This means that the method used to prove that the $V_{SS} = 0$ condition results in a legitimate discretization cannot be used if we use the $X = \log S$ transformation. Nevertheless, it is possible to use more complex methods, such as those described in [20] to show that this boundary condition applied to equation (7.1) is legitimate.

Suppose that we have an underlying asset (such as an interest rate, or a commodity) which cannot be stored at no cost. If

$$dS = a(S,t)\ dt + b(S,t)\ dZ \tag{7.2}$$

then standard methods can be used to give the value $V(S,t)$ of a contingent claim on S as the solution to

$$V_\tau = \frac{b^2}{2} V_{SS} + (a - \lambda b) V_S - rV \tag{7.3}$$

where λ is the market price of risk. This example would include the common situation of mean reversion, i.e.

$$a = \kappa(\theta - S) \ \ ; \ \ \theta, \kappa \geq 0 \ \ . \tag{7.4}$$

In this case, if we have the condition

$$\begin{aligned} b &\to 0 \ \ ; \ \ S \to 0 \\ b &\leq C_2 S \ \ ; \ \ S \to \infty \\ a - \lambda b &\geq 0 \ \ ; \ \ S \to 0 \\ a - \lambda b &\leq 0 \ \ ; \ \ S \to \infty \end{aligned} \tag{7.5}$$

then it is easy to show that imposing $V_{SS} = 0$ at $S = S_{max}$, and using one sided differencing at $S = 0, S = S_{max}$ results in a method which is unconditionally stable if fully implicit timestepping is used, and is at least algebraically stable if Crank-Nicolson timestepping is used. If the conditions (7.5) do not hold, then it would be necessary to precisely examine the properties of a, b in each case to determine if the methods in [20] could be used to determine if a legitimate discretization is obtained.

8. Conclusions. In this paper we have provided an analysis of the stability of the linear boundary condition for the Black-Scholes equation. New financial contracts are being continually invented. Imposing Dirichlet type conditions for each of these new contracts would be a tedious complication in a software library. Use of the linear boundary condition avoids this difficulty, and perhaps explains why the use of this boundary condition is popular among practitioners. However, to our knowledge there have been no studies which examine the stability of this boundary treatment.

We defined the notion of a legitimate discretization, which requires that the discrete spatial operator preserves certain spectral properties of the continuous spatial operator. It was shown that the legitimate spatial discretizations given in this paper result in fully implicit and Crank-Nicolson timestepping algorithms that satisfy necessary conditions for stability when $r > 0$. The linear boundary condition results in a legitimate discretization for a FD method described in this paper.

We also provide a numerical example for which the PDE boundary condition does not result in a legitimate discretization. As a result, the discrete equations can exhibit growth which is not consistent with the governing equations. In our experience, we observe that the PDE boundary condition can be applied to many situations without introducing instability. However, we suggest that this asymptotic condition is applied with care.

It is difficult to provide sufficient conditions which guarantee that the linear boundary condition results in a stable discretization when $r - q > 0$. We provided numerical examples which demonstrate that the linear boundary condition results in a discretization that is power-bounded in a wide variety of situations, assuming that the volatility is bounded away from zero, $\sigma \geq \sigma_0 > 0$. We also provided heuristic reasoning that indicates why we might not expect to observe difficulties applying the linear boundary condition, even in the extreme case when $\sigma = 0$.

REFERENCES

[1] R. Bhatia, *Matrix Analysis*, Springer Verlag, 1997.
[2] N. Borovykh, D. Drissi, and M. N. Spijker, *A bound on the powers of linear operators, with relevance to numerical stability*, Applied Mathematics Letters, 15 (2002), pp. 47–53.
[3] N. Borovykh and M. N. Spijker, *Resolvent conditions and bounds on the powers of matrices, with relevance to the numerical stability of initial value problems*, Journal of Computational and Applied Mathematics, 125 (2000), pp. 41–56.
[4] Y. d'Halluin, P. A. Forsyth, and K. R. Vetzal, *Managing capacity for telecommunications networks under uncertainty*, IEEE/ACM Transactions on Networking, 10 (2002), pp. 579–588.
[5] M. B. Giles, *On the stability and convergence of discretizations of initial value PDEs*, IMA Journal of Numerical Analysis, 17 (1997), pp. 563–576.
[6] R. Kangro and R. Nicolaides, *Far field boundary conditions for Black-Scholes equations*, SIAM Journal on Numerical Analysis, 38 (2000), pp. 1357–1368.
[7] J. F. B. M. Kraaijevanger, H. W. J. Lenferink, and M. N. Spijker, *Stepsize restrictions for stability in the numerical solution of ordinary and partial differential equations*, Journal of Computational and Applied Mathematics, 20 (1987), pp. 67–81.
[8] H. W. Lenferink and M. N. Spijker, *On the use of stability regions in the numerical analysis of initial value problems*, Mathematics of Computation, 57 (1991), pp. 221–237.

[9] D. Levy and E. Tadmor, *From the semidiscrete to fully discrete: Stability of Runge Kutta schemes by the energy method*, SIAM Review, 40 (1998), pp. 40–73.
[10] M. D. Marcozzi, *On the approximation of optimal stopping problems with applications to financial mathematics*, SIAM Journal on Scientific Computing, 22 (2001), pp. 1865–1884.
[11] K. W. Morton, *Stability of finite difference approximations to a diffusion-convection equation*, International Journal for Numerical Methods in Engineering, 15 (1980), pp. 677–683.
[12] ———, *Numerical Solution of Convection-Diffusion Problems*, Chapman & Hall, 1996.
[13] O. A. Oleinik and E. V. Radkevic, *Second Order Equations with Nonnegative Characteristic Form*, American Mathematical Society, Providence, R.I., 1973.
[14] R. D. Richtmyer and K. W. Morton, *Difference Methods for Initial-Value Problems*, Interscience Publishers, 1967.
[15] E. Sousa and I. Sobey, *On the influence of numerical boundary conditions*, Applied Numerical Mathematics, 41 (2002), pp. 325–344.
[16] M. N. Spijker and F. A. J. Straetemans, *Error growth analysis via stability regions for discretizations of initial value problems*, BIT, 37 (1997), pp. 442–464.
[17] F. A. J. Straetmans, *Resolvent conditions for discretizations of diffusion-convection reaction equations in several space dimensions*, Applied Numerical Mathematics, 28 (1998), pp. 45–67.
[18] D. Tavella and C. Randall, *Pricing Financial Instruments: The Finite Difference Method*, John Wiley & Sons, Inc., 2000.
[19] P. Wilmott, *Derivatives*, John Wiley and Sons, West Sussex, England, 1998.
[20] H. Windcliff, Numerical Methods for complex path dependent options. PhD Thesis (Computer Science), University of Waterloo, 2003.
[21] H. Windcliff, P. A. Forsyth, and K. R. Vetzal, *Segregated funds: Shout options with maturity extensions*, Insurance, Mathematics & Economics, 29 (2001), pp. 1–21.
[22] ———, *Shout options: A framework for pricing contracts which can be modified by the investor*, Journal of Computational and Applied Mathematics, 134 (2001), pp. 213–241.
[23] R. Zvan, P. A. Forsyth, and K. R. Vetzal, *Negative Coefficients in Two Factor Option Pricing Models*. to appear in the Journal of Computational Finance.